MOLECULAR DYNAMIC SIMULATION OF POOL BOILING PROCESS

BY

KATARZYNA BOROWIEC

THESIS

Submitted in partial fulfillment of the requirements
for the degree of Master of Science in Nuclear, Plasma, and Radiological Engineering
with a concentration in Computational Science and Engineering
in the Graduate College of the
University of Illinois at Urbana-Champaign, 2017

Urbana, Illinois

Master's Committee:

Associate Professor Tomasz Kozlowski
Assistant Professor Yang Zhang

Abstract

Following work presents molecular dynamic simulation of the pool boiling process of water molecules with heater modelled as lattice of copper atoms. Heat transfer coefficient was calculated, and the results were compared to existing correlations for pool boiling heat transfer. The purpose of the analysis was to test feasibility of molecular dynamics simulation in the study of boiling process. Using approximate potentials, methodology of molecular dynamics simulation applied to boiling process was presented. The results may be improved with the use of more sophisticated description of molecular interactions, increasing domain size and time of the simulation. Due to limitation of the analysis accurate prediction of heat transfer coefficient was not possible.

In this work, temperature of the heated surface was controlled variable and the value of heat flux was measured. Simulation was conducted for water at pressure 2.7 bar, which is typical pressure of reflood and passive cooling systems. The bulk of the water was kept at saturation temperature for the entirety of simulation. Temperature of the heated surface was set to achieve desired temperature difference between saturated fluid and wall equal to $\Delta T = [10, 20, 30, 40]\mathrm{K}$. Heater was modelled as copper atoms arranged in the lattice with Morse potential governing the interac-

tion. Potential between water molecules was represented using TIP4P/2005 model [1] and water-copper interaction was set to be Lennard-Jones potential. Simulation was conducted with the use of LAMMPS molecular dynamic simulator [2] [3].

Analysis included investigation of potentials for water by surface tension and liquid - vapor density calculation. Water-copper interaction was parametrized based on contact angle of water droplet on the copper surface.

Analysis of pool boiling indicated a significant difference between heat transfer coefficient calculated from simulation and the value calculated form the available correlations. This discrepancy is caused by inaccurate representation of potential between water molecules and the atoms of the copper surface, underlying differences in surface properties and differences in macroscopic and microscopic phenomena. Additionally, analysis was limited in size of the system and time of the simulation, which makes comparison with experimental results not feasible. Nevertheless, presented work gives framework for further study of heat transfer on microscopic level.

Acknowledgments

I would like to express my appreciation to Professor Kozlowski, my thesis advisor, for his guidance, support and encouragement during my research work. His help and commitment motivated me through the process of writing this thesis.

I would like to acknowledge Professor Zhang as the second reader of this thesis. His valuable comments helped me greatly in preparation of final version of my thesis.

I want to thank all the members of Analysis of Reactor Transients and Stability (ARTS) group for help and inspiration throughout my study and UIUC. My grateful thanks to all NPRE department staff and faculty whose support and encouragement made this work possible.

Finally, I must express my utmost gratitude to my parents and to my sister for providing me with encouragement and constant support throughout my study and through the process of writing this thesis. This achievement would not have been possible without their continuous help. Thank you very much.

Table of Contents

List of Tables

List of Figures

List of Abbreviations

CA	Contact Angle
HT	Heat transfer
MD	Molecular Dynamics
G	Gorenflo
C	Cooper
M	Mostinski

List of Symbols

A	Area
d	Number of degrees of freedom per atom
f	Force
h	Heat transfer coefficient
k	Boltzmann constant
m	Mass
M	Molecular mass
n	Number of molecules (atoms)
N_a	Avogadro's number
q	heat transfer
U	Potential
V	Volume
ϕ	Potential
γ	Surface tension
E_k	Kinetic energy
p_{crit}	Critical pressure
R	Wall roughness

Chapter 1

Introduction

Computer simulation have been used as a tool to decrease the need for costly experiments or to supplement their findings. While experiments requiring extreme values of pressure and temperature are very difficult to perform, it requires the same computational effort regardless of the test conditions.

Molecular dynamic (MD) simulations were proven successful in many disciplines. With a simple underlying idea of solving Newton's equation of motion for every molecule in the system, MD simulation found broad application in biology [5], material science [6], heat transfer [7] and other fields. It was shown that MD simulations can accurately predict macroscopic properties of the system [8] [9]. That gives a possibility to investigate processes on molecular level and solve problems requiring microscopic approach. Nevertheless, MD has considerable spatial and temporal limitations due to computational cost. For each time step, potential for each atom must be calculated, dependent on all positions of all remaining atoms in the system. Increasing computational power, increases the size and time domains for which simulations can be performed.

Introduction of faster algorithms and simplifications decreases computational effort. Nevertheless, it remains significant giving limitations to simulation time and

size of the system under investigation, due to number of operations that need to be performed. With ever-growing computational resources and clever application of boundary conditions, results of some of the simulations can be compared to macroscopic values.

The underling challenge is to find the interaction potential that will model essential physics of the phenomena but would not be computationally expensive. There are multiple potentials that are suitable for different simulations. Molecular dynamics was coupled to continuum mechanics [10] and can be used together with Monte Carlo methods [11].

Two-phase flow is critical in description of many industrial processes. In nuclear engineering, modelling of BWR normal operation and PWR accidents scenarios require accurate models of two phase heat transfer. Decreasing size of high performance microelectronics need more efficient way of cooling. Utilization of the phase change is one of the ways heat transfer can be increased. Two phase flow is utilized in chemical reactor to promote mixing or to improve reaction kinetics. Wellbore gas influx is modelled with two-phase flow in oil industry. Additionally, multiple gas injection systems exist in engineering application such as relive valves in refrigeration systems.

Pool boiling is the most basic form of two-phase flow and heat transfer. It is characterized by the presence of the heating surface immersed in large body of liquid and at the temperature above saturation temperature of the liquid. It is encounter in various industrial applications. For that reason, multiple correlations were created to calculate heat transfer coefficient for pool boiling. Additionally, in some computer codes such as TRACE, nucleate boiling heat transfer coefficient is calculated as an

linear superposition of forced convection and pool boiling [12].

Application of molecular dynamic simulations to investigate heat transfer phenomenon seems particularly appealing for nanotechnology. Nevertheless, attempts were also made to investigate large scale phenomena such as phase change where MD simulation may help in understanding liquid-solid interaction, nucleation and effect of surfactants [13]. All of those phenomena include microscopic effects that can be studied with MD. The biggest challenge in performing accurate MD simulations are spatial and temporal limitations as well as assigning potentials that are not computationally expensive but still model the essential physics. Despite those limitations, MD simulations were successfully utilized in phase change process and heat conduction problems [13].

Some applications of molecular dynamics requires inclusion of quantum mechanics consideration which can be done with "ab initio" methods that relay on solution of approximate Schrödinger equation. Nevertheless, although theoretically correct, those type of simulations have even bigger constraints in terms of number of particles and time of the simulation, typically limited to system of 10-100 atoms. Most of the potentials have semi-empirical form that is adjusted to fit experimental data. Then, those potentials are validated on the property which was not used in the fitting process. Surface tension is common choice in measuring the performance of a given potential. For Lennard-Jones fluid accurate predictions were achieved by [14, 15]. Studies of the surface tension was also used in comparison and assessment of water potentials [16, 17] .

Molecular dynamics simulations found wide application in study of heat transfer.

Most of the work in MD heat transfer was focused on investigation of nanofluids and nanostructures. Comprehensive review of the heat transfer from nanoparticles can be found in [18]. The MD simulations are considered a perfect tool for study of nanoparticle behaviour due to the scale of phenomena that could not be captured by classical theory. Effective thermal conductivity was studied using MD simulation and enhanced thermal transport was realized in [19]. Possibility of heat transfer enhancement by introduction of nanofins on the surface was investigated by Tang at al. (2014) .

Phase change was widely studied in MD simulations. Hens at al. (2014) studied evaporation of liquid argon film on platinum surface [20]. Additionally, the bubble formation was investigated with different surface properties. It was shown that bubbles are less likely to form on a non-wetting surface. It was concluded that bubble is easily formed at higher degree of superheats. Simulation of bubble creation was performed and its properties investigated [21, 22]. Park at al. investigated surface tension of bubbles and their characteristics. It was shown that surface tension of droplets varies according to Tolman's equation but for bubbles it is greater by 15% or less. Okumura and Ito (2003) showed agreement of macroscopic theory of Rayleigh-Plasset equation and molecular dynamic simulation of bubble dynamics, proving hydrodynamic description is reliable even in microscopic bubble.

Attempts have been made to calculate heat transfer coefficient (HTC). HTC was determined with MD simulation for argon between two copper plates, where one was stationary and other was moving with some velocity [23]. The result was compared to analytical solution with correction to account for nanoparticles. Authors reported

parabolic velocity profile and linear temperature profile. The calculated HTC was lower then analytical solution but of the same order of magnitude. Influence of nanofluid presence on pool boiling heat transfer coefficient was investigated in [24]. Authors observed enhanced heat transfer with enhancement more pronounced for higher heater temperatures. Additionally, different placement of nanoparticle was investigated. Effect was more pronounced for nanoparticle placed near the wall rather than away from the wall.

The heat transfer coefficient for pool boiling was simulated for Lennard-Jones liquid with successful observation of different flow regimes. The simulation used 484 thousand particles that were modelled as argon atoms [25]. Nevertheless, computed heat transfer coefficient could not be compared with experimental data. The size of domain was limited to micrometer range and short cut off was applied, to work within the constraints of computational limitation. However, no attempt of simulating pool boiling heat transfer coefficient for water is known to the author. The level of difficulty increases as potential describing behavior of water is more computationally expensive, limiting simulation domain even further.

Chapter 2

Theory

2.1 Molecular Dynamic Simulation

MD simulation relies on numerical solution of Newton's equation of motion. It can be written as [26]:

$$m_i \frac{d^2 r}{dt^2} = f_i \tag{2.1}$$

Force is represented by the potential $f_i = -\frac{\partial}{\partial r_i} U(r^n)$, where r^n is representing positions of all the atoms in the system. Potential is calculated based on positions of all the other atoms in the simulation domain and their relative position, which makes it computationally expensive when number of atoms is large. In practical applications for non-bounded interactions, only externally applied potential field and pair potential are considered, three-body and higher terms are neglected. This approach gives good results for many applications. Bonds in the molecules can be modelled with special bonding potentials such as harmonic oscillator or by rigid bounding which assures the distance between atoms remains constant.

Solution of the equation 2.1 is done in the simplest possible way to decrease the computational effort. One of the commonly used algorithms is "Leapfrog Verlet"

algorithm. The solution for velocity and position is summarised in Eq. 2.2.

$$\begin{aligned} v_{i+1/2} &= V_{i-1/2} + \delta_t \frac{F(x_i)}{m} \\ x_{i+1} &= x_i + \delta_t v_{i+1/2} \end{aligned} \tag{2.2}$$

Even with such simple integration scheme calculations are computationally expensive due to:

- Short time step required for simulation (on the order of 10^{-15}s).
- Calculations need to be repeated multiple times to achieve required time scale.
- Depending on the number of atoms in the systems significant amount of calculations need to be performed. Non-bounded interaction act between every pair of atoms.

Multiple methods were utilized to decrease the computational effort. From faster algorithms, to approximate methods. To reduce number of computations, interactions of atoms above certain distance are ignored, which is good approximation for some interaction types. Number of required atoms in the system can be decreased by introduction of periodic boundary conditions which prove to be successful in determination of material properties.

There are different type of ensembles that can be used when performing the simulation:

- **NVT** - canonical ensemble - where number of atoms, volume and temperature are kept constant.

- **NVP** - isobaric-isothermal ensemble - where number of atoms, pressure and volume are constant.
- **NPH** - isobaric-isoenthalpic ensemble - where number of atoms, pressure and enthalpy is fixed.
- **NVE** - microcanonical ensemble - where number of atoms, volume and total energy is conserved.

2.2 Thermodynamic properties in MD

Molecular dynamics simulation relies on statistical thermodynamics to determine basic thermodynamic properties of the system. Most of the properties of the system can be computed based on position and forces acting between particles. This section describes methods of calculating required properties and basic ideas about MD simulations.

Density of atoms can be computed directly from the definition. Method of calculating density of atoms in cubic volume with sides $[L_x, L_y, L_z]$ is presented in Eq. 2.3

$$\rho = \frac{nM}{N_a L_x L_y L_z} \tag{2.3}$$

The temperature of the system can be calculated by kinetic energy of the system as in Eq. 2.4.

$$T = \frac{2E_k}{ndk} \tag{2.4}$$

The kinetic energy of the system is calculated as the average kinetic energy of all of

atoms in the system:

$$E_k = \sum_{i=0}^{n} \frac{1}{2} m_i v_i^2 \tag{2.5}$$

The pressure tensor for the system can be calculated from the positions and velocities according to Eq. 2.6.

$$P_{xy} = \frac{1}{V}[\sum_j m_j v_{xj} v_{yj} + \frac{1}{2} \sum_{i,i\neq j} \sum_j r_{xij} f_{uij}] = \frac{1}{V}[\sum_j m_j v_{xj} v_{yj} + \sum_{i>j} \sum_j r_{xij} f_{yij}] \tag{2.6}$$

The system surface tension can be calculated with Eq. 2.7.

$$\gamma = \sum_{i>j} \sum_j \frac{x_{ij}^2 + y_{ij}^2 - 2z_{ij}^2}{2Ar_{ij}} \tag{2.7}$$

To calculate heat transfer coefficient for pool boiling the heat flux from the heater to water needs to be estimated. The heat flux in MD simulation can be expressed as:

$$\mathbf{J} = \frac{1}{V}\Big[\sum_i e_i v_i + \frac{1}{2} \sum_{i<j} (f_{ij} \cdot (v_i + v_j)) x_{ij}\Big] \tag{2.8}$$

The positions of atoms are governed by stochastic behaviour. For that reason, final estimate of the thermodynamic quantity is based on the time average over multiple timesteps. The accuracy of the estimate will depend on the averaging period. Because the simulation starts at arbitrary state, some time is necessary for system to equilibrate before the data can be collected.

2.3 Potentials

Results of the simulation are strongly dependent on applied potential. One of the simplest potentials is the Lennard-Jones potential. The functional representation is shown in Eq. 2.9, where σ_{LJ} represents intermolecular distance at which potential between particles is zero and ϵ_{LJ} determines depth of potential well.

$$\phi_{LJ}(r) = 4\epsilon_{LJ}\left[\left(\frac{\sigma_{LJ}}{r}\right)^{12} - \left(\frac{\sigma_{LJ}}{r}\right)^{6}\right] \tag{2.9}$$

L-J potential is most commonly used to describe interaction of noble gases with great success. In the following work this potential was used to model water - copper interaction due to its simplicity. Description of potential for water molecule is more complicated as interaction between the particles inside the molecules must be included. The description of water and copper potential used in the simulation is presented in Chapter 3.

2.4 Pool boiling

Pool boiling occurs when solid surface is immersed in large body of liquid at rest and its temperature is higher than saturation temperature of the liquid. It is the simplest form of the two-phase flow. During pool boiling bubbles will start to form near the surface as phase change process will occur. Example of the boiling cure is presented in Fig. 2.1. In the figure heat flux q'' versus temperature difference ΔT is plotted. ΔT is defined as the difference of heated surface temperature and

saturation temperature of the liquid. The curve is different for different fluids at different pressures. Additionally, the geometry and surface roughness may influence the shape of the curve. Experimental pool boiling curve can be obtained using two different approaches. Either temperature or heat flux can be controlled while the other quantity is measured. Boiling process has different characteristics dependent on temperature difference [4]:

- Region I: Corresponds to natural convection, where no bubbles are formed, and heat is transferred from heated surface to liquid only through natural convection.

- Region II: Nucleate boiling region, as temperature increases bubbles start being generated at nucleation sites. At lower values of ΔT bubbles can grow and detach without interaction with other bubbles. Further increase in temperature difference causes more generation sites to be activated. More bubbles are created and will merge creating columns or slugs of vapor decreasing the contact area between liquid and solid surface. The flux eventually achieves maximum value (point C), value of heat flux corresponding to this point is called the critical heat flux.

- Region III: Transition boiling, further increase in temperature causes bubbles to be generated faster than they can detach from the surface. As they merge, film of vapor is created on the heating surface decreasing efficiency of heat transfer. This process is unstable due to possibility of film detachment. With increasing temperature, a stable film is created, and heat flux achieves its minimum value

at point D.

- Region IV: Film boiling, after point D phase change occurs at the interface between liquid and vapor and heat is transferred by convection in the vapor film and through radiation.

- For heat flux controlled system: Curve goes directly from point C to point E. When critical heat flux is exceeded temperature of the solid surface rapidly increases as heat transfer coefficient is drastically decreased.

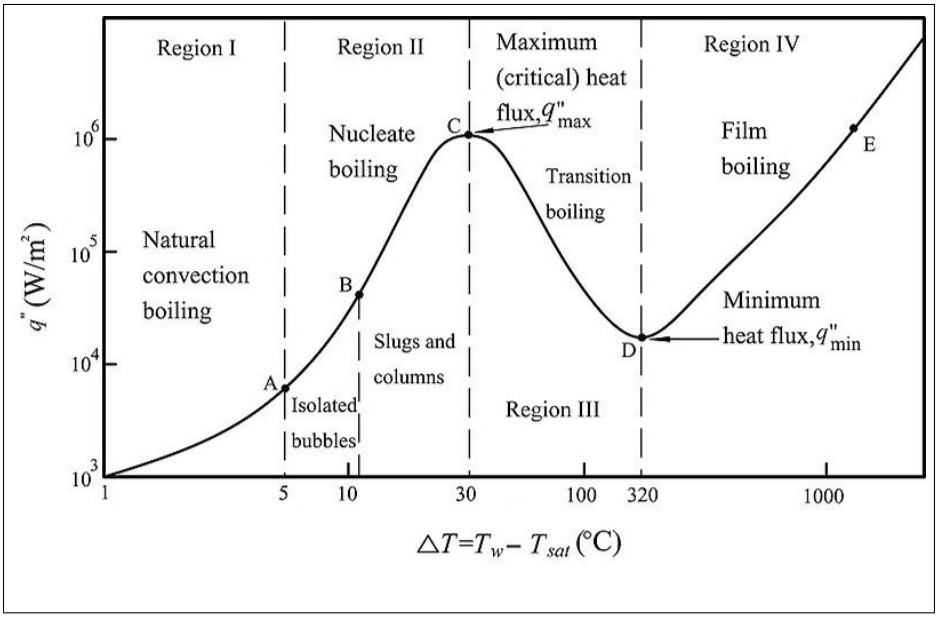

Figure 2.1: Pool boiling curve [4] for water at atmospheric pressure with temperature controlled system.

Pool boiling curve in practical applications such as computer codes is implemented using available correlations. Same of the existing correlations are Gorenflo [27], Cooper [28], Mostinski [29]. Those correlation were chosen for the comparison be-

cause those do not depend on the geometry. Nevertheless, those semi empirical models lack generality and do not give good predictions for wide range of conditions. The correlation themselves are not consistent and give different predictions as illustrated in Fig. 2.2. Due to lack of experimental data the comparison of the correlations is difficult. Those correlations are presented below, where $p_r = \frac{p}{p_{crit}}$.

Gorenflo correlation

$$h_C^G = h_0 F_g \Big(\frac{q}{q_0}\Big)^n \Big(\frac{R}{R_0}\Big)^{0.133} \tag{2.10}$$

where $F_g = 1.73 p_r^{0.27} + \Big(6.1 + \frac{0.68}{1-p_r}\Big) p_r^2$ and $n = 0.9 - 0.3 p_r^{0.15}$.

With constants:

$h_0 = 5600 \frac{W}{m^2 K}$,

$q_0 = 20000 \frac{W}{m^2}$,

$R_0 = 0.4 \mu m$.

Cooper correlation

$$h_C^C = 55 p_r^{0.12 - 0.4343 ln R} (-0.4343 ln p_r)^{-0.55} M^{-0.5} q^{0.67} \tag{2.11}$$

Mostinski correlation

$$h_C^M = 0.00417 q^{0.7} p_{crit}^{0.69} F_m \tag{2.12}$$

where $F_m = 1.8 p_r^{0.17} + 4 p_r^{1.2} + 10 p_r^{10}$.

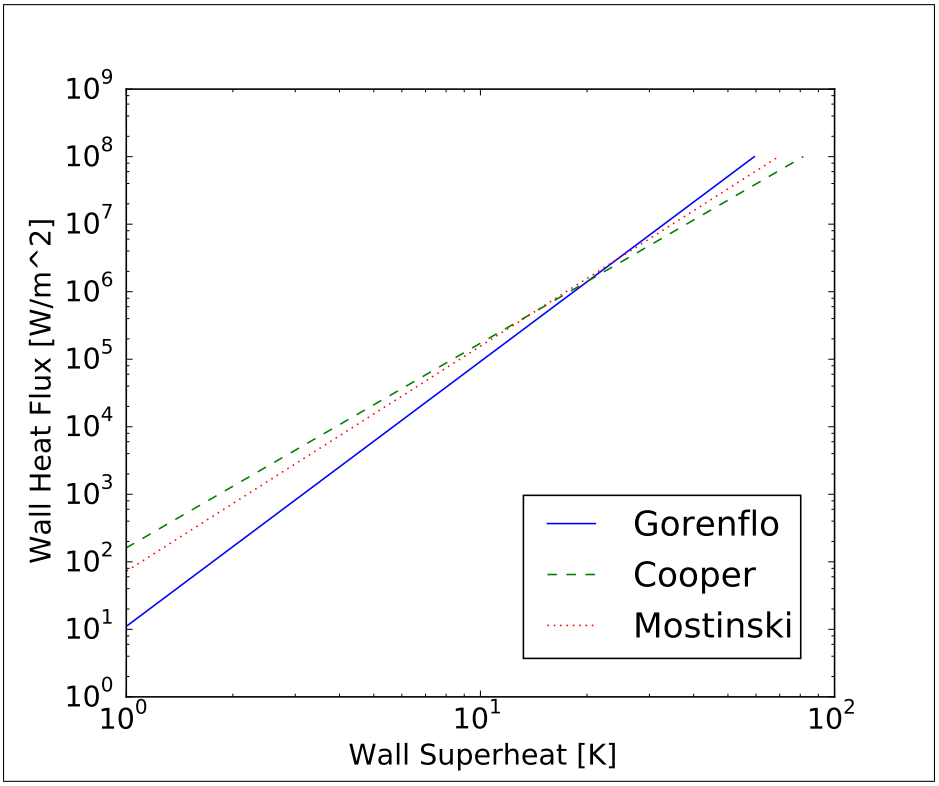

Figure 2.2: Comparison of different correlations for pool boiling heat transfer coefficient for water at p = 2.7bar. Correlation of Gorenflo, Cooper and Mostinski are presented.

Chapter 3

Results

MD simulation results depend strongly on potential used for the analysis. It is required to model essential physics of the phenomena while economizing computational resources. The analysis has been made to investigate potential performance in determining macroscopic properties. Water potential TIP4P/2005 [1] was used to predict surface tension, density of liquid and vapor phase. Results of the simulation were compared to experimental values. Copper interaction with water potential was adjusted to accurately represent contact angle of the droplet on copper plate.

3.1 Modelling of interactions between atoms

Modelling interactions of water molecules is more complicated than the noble gas that can be successfully simulated with the Lennard-Jones potential. The main challenge is representation of a strong, directional hydrogen bonds [30]. TIP4P/2005 potential for water molecule interaction was chosen. In this model molecule is represented by four sites. Two sites are occupied by hydrogen atoms with positive charges. Third site is occupied by Oxygen atom and fourth by negative charge. Interaction has Lennard-Jones part and Coulombic part that acts between all intermolecular pairs.

Functional representation of this model,

$$U_{12} = 4\epsilon\Big[\Big(\frac{\sigma}{r}\Big)^{12} - \Big(\frac{\sigma}{r}\Big)^{6}\Big] + \sum_j \sum_i c\frac{q_i q_j}{r_{ij}}, \tag{3.1}$$

where ϵ represents interaction strength, σ interatomic separation, r is a distance and q charge. Parameters for the model are presented in Table 3.1. The geometry of the water molecule model is presented in Fig. 3.1.

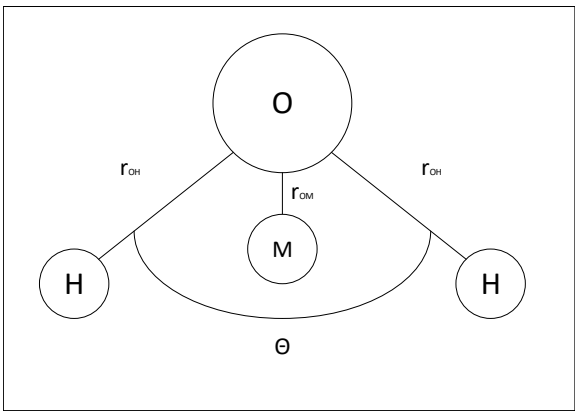

Figure 3.1: Geometrical representation of water molecule in TIP4P model. M represents position of the negative charge.

Morse potential was chosen for copper interaction because it is relatively computationally inexpensive and simple. Interaction of liquid with solid surface is of greatest interest in this study, and interactions between atoms in the surface are not that important. Therefore, interactions of surface atoms were modelled with simple potential to decrease computational effort. The general form,

$$U = D\Big[e^{-2\alpha(r-r_o)} - 2e^{-\alpha(r-r_o)}\Big], \tag{3.2}$$

Table 3.1: Model parameters for TIP4P potential

TIP4P Model parameters	
$\sigma_{OO}[\mathring{A}]$	3.1589
$\epsilon_{OO}[\frac{kcal}{mol}]$	0.1852
$\sigma_{HH}, \sigma_{OH}[\mathring{A}]$	0.00
$\epsilon_{HH}, \epsilon_{OH}[\frac{kcal}{mol}]$	0.00
$q(O)$	-1.1128
$q(H)$	0.5564
$q(M)$	-1.05
$r_c[\mathring{A}]$	13.00
$\angle OHO$	104.52
$R(OH)[\mathring{A}]$	0.9572
$R(M)[\mathring{A}]$	0.1546

Table 3.2: Model parameters for Morse potential

Morse potential parameters	
$\alpha[\mathring{A}^{-1}]$	1.36
$D[\frac{kcal}{mol}]$	7.91
$r_0[\mathring{A}]$	2.87

were D represents interaction strength, r_o - equilibrium length, α constant. Parameters used for Morse potential are summarized in Table 3.2. Lattice constant that was used to determine the initial positions of copper atoms in the simulation is $a = 3.62\mathring{A}$. Biggest challenge remains in prescribing correct potential to interaction of water molecules and copper atoms. To minimize computational effort the simplest potential was chosen, namely Lennard-Jones potential with parameters chosen to give contact angle in agreement with experimental value. The parameters that were chosen are presented in Table 3.3.

Table 3.3: Model parameters for Lennard-Jones potential.

Lennard-Jones potential	
$\sigma_{HCu}[\mathring{A}]$	2.373
$\sigma_{OCu}[\mathring{A}]$	2.886
$\epsilon[\frac{kcal}{mol}]$	0.15

3.2 Prior Analysis

Surface tension was calculated with Eq. 2.7. Design of the initial state of the system is presented in Fig. 3.2. Cube of water molecules arranged in lattice with free space along one direction equal to the side of the cube. All of the boundaries were set as a periodic boundary condition. The simulation was performed with lattice of 22x22x22 water molecules, with time step 1fs. Simulation was run for about 200 000 timesteps with 50 000 timesteps allowed for thermalization. Thermostat was placed on the system for the entirety of the simulation.

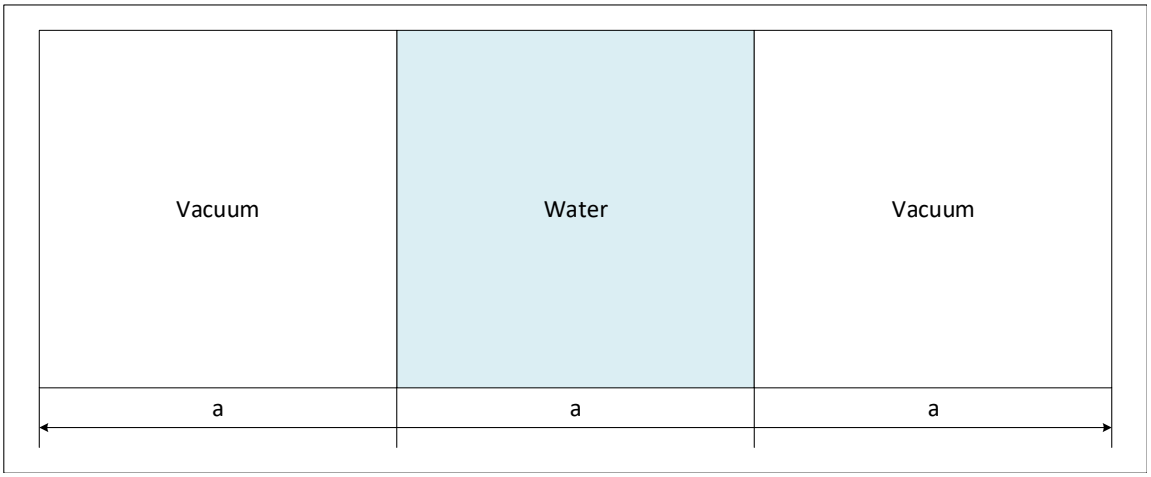

Figure 3.2: Simulation setup for calculation of surface tension.

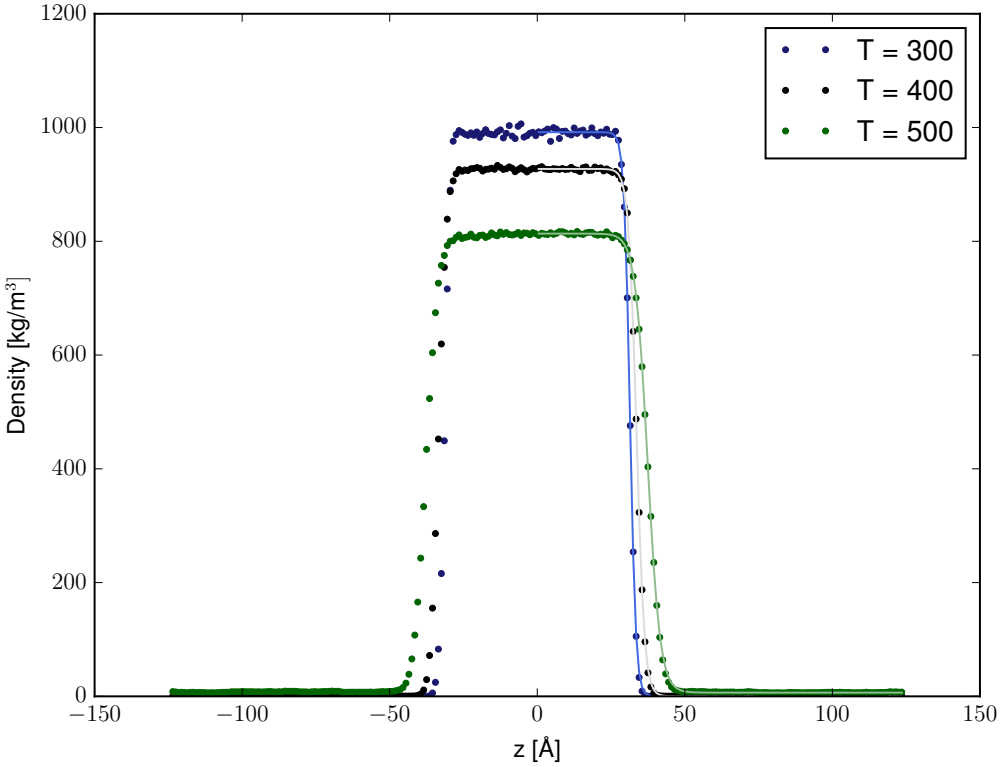

Figure 3.3: Density profiles along simulation box.

Density of the simulation was evaluated by fitting function in Eq. 3.3 to the density profile, as shown in Fig. 3.3. Simulation values and steam table values are presented in Fig. 3.4.

$$\rho(z) = \frac{1}{2}(\rho_l + \rho_v) + \frac{1}{2}(\rho_l - \rho_v)tanh(\frac{z - z_o}{d}) \tag{3.3}$$

The simulation gives accurate estimation of liquid and vapor densities especially for lower values of temperature. The simulation of surface tension accurately represents

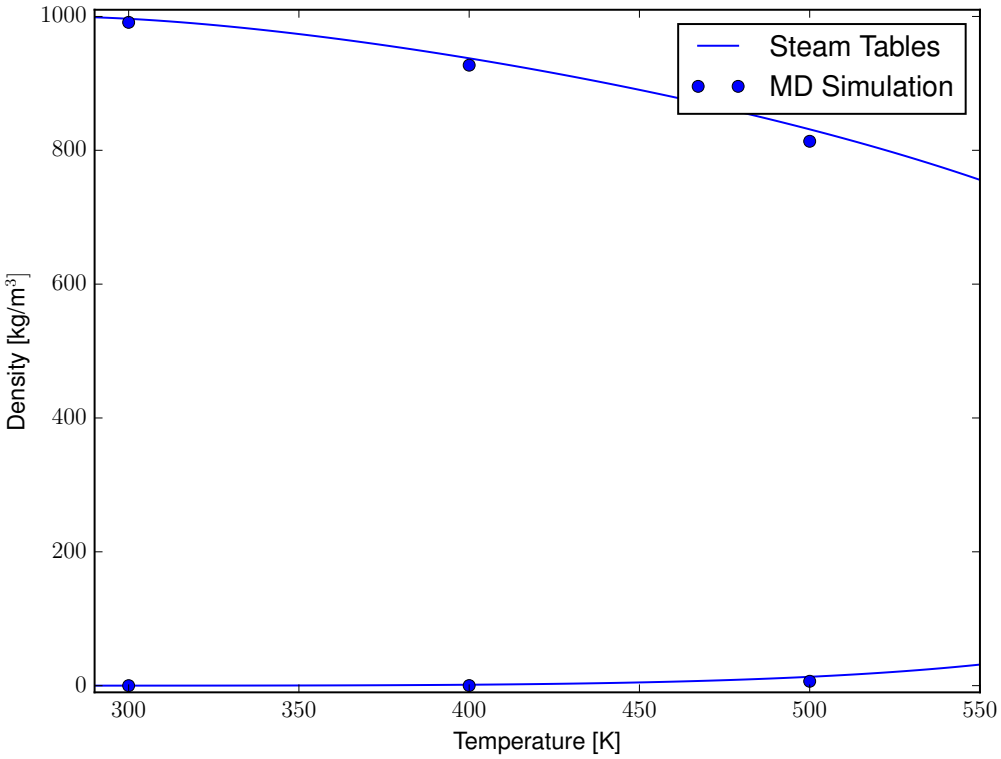

Figure 3.4: Comparison of calculated density for gas and liquid phase with steam table values.

the trend of surface tension as a function of temperature. Nevertheless, values predicted by the model are noticeably lower than the experimental values. The reason for this discrepancy is caused by a limited number of water molecules. The increase in accuracy can be achieved by increasing number of water molecules inside the system. Numerical values of density and surface tension calculation are presented in Table 3.4.

To determine appropriate potential between copper atoms and water molecules

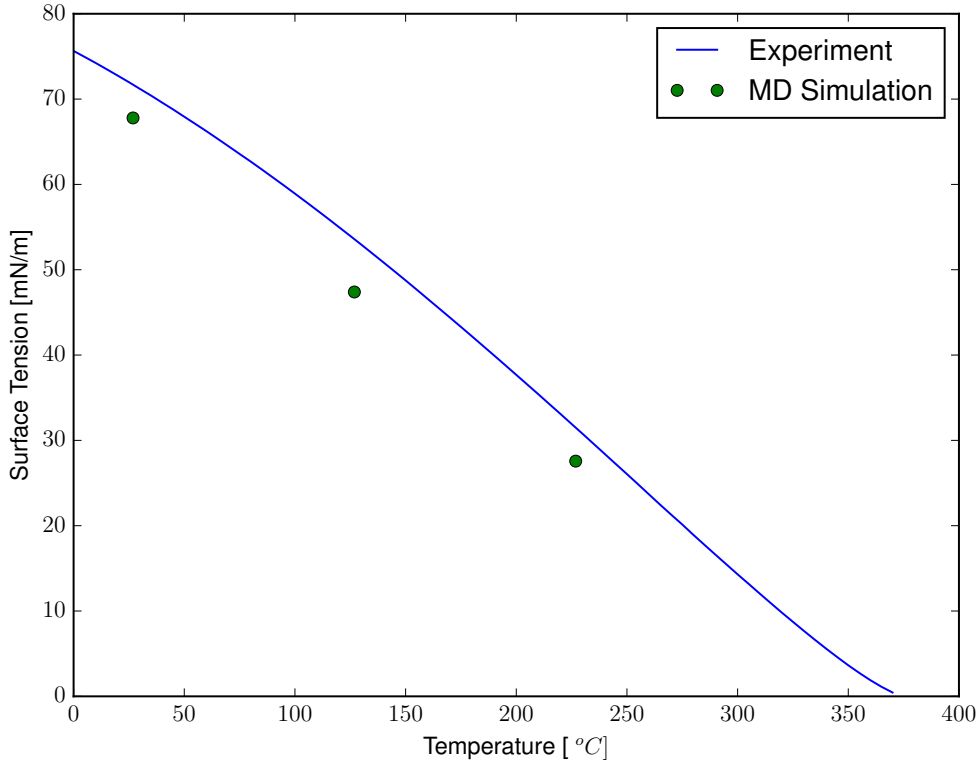

Figure 3.5: Surface tension comparison for simulation and experimental results.

Table 3.4: Validation of water TIP4P potential.

Density

T [K]	$\rho_l^{MD}[\frac{kg}{m^3}]$	$\rho_l^{ST}[\frac{kg}{m^3}]$	$\rho_g^{MD}[\frac{kg}{m^3}]$	$\rho_g^{ST}[\frac{kg}{m^3}]$
300	991.19	996.51	0.0	0.03
400	927.18	937.48	0.13	1.37
500	813.47	831.32	6.54	13.20

Surface Tension

T [K]	$\gamma^{MD}[\frac{mN}{m}]$	$\gamma^{E}[\frac{mN}{m}]$	
300	67.79	71.69	
400	47.39	53.58	
500	27.57	31.49	

contact angle simulation was performed. Simulation domain consisted of plate created out of copper atoms arranged in a lattice. Cube of water molecules 15x15x15, was placed above the plate for the initial state to prevent disintegration of copper plate, initial state of the system is visualized in Fig. 3.6. After system thermalized the contact angle was measured, modified approach of [31] was employed. The simulation domain consisted of 16810 copper atoms and 3375 water molecules. System was allowed to equilibrate for 420000 and data was collected for additional 300000 time steps. Simulation was performed with 2fs time step. Temperature of T = 100^{o}C was kept constant through the simulation with application of a thermostat.

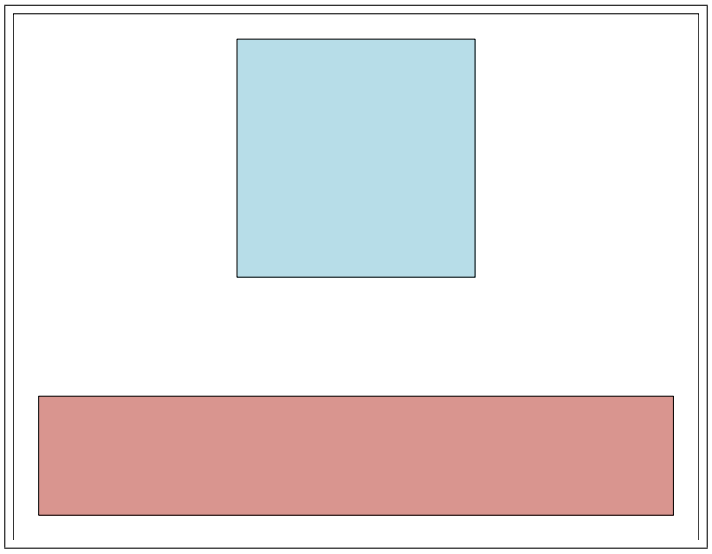

Figure 3.6: Initial state for contact angle simulation. Cube of water molecules was placed above the lattice composed of copper atoms.

Simulation provided position of all particles in the system for different timesteps. Distribution of atoms in the system was averaged over time. Next, the domain was divided in z direction. For each elevation radial distribution was calculated,

Table 3.5: Comparison of experimental contact angle of water droplet on copper plate with simulation results.

MD CA	Experimental CA [32]
71.62	72.00

example of the distribution is shown in Fig. 3.7. Transition between liquid and the vapor phase was identified for each bin and plotted in r-z space as indicated in Fig. 3.8. Transition was defined as the point where fitted function changed curvature, function in Eq. 3.3 was fitted to radial density profile to identify the change. Circle equation was fitted to the points and the tangent line was drown at the beginning of the droplet. Due to instability of the layer near the surface, transition at some of the lower elevations could not be determined, those points were omitted. Resulting contact angle and experimental value at T=100^{o}C are presented in Table 3.5.

It is worth mentioning that potential was fitted for only one value of temperature. Contact angle at high temperature was chosen because the simulation of the pool boiling is performed in higher temperature. Nevertheless, potential for water copper interaction is only rough approximation of the true interaction. For more accurate model of interaction of water with metal surface induction of charges inside the conductor by water molecules should be included as an additional term. This phenomenon was not modelled in the following analysis to decrease computational effort.

The findings of this analysis were used to develop simulation of pool boiling heat transfer coefficient.

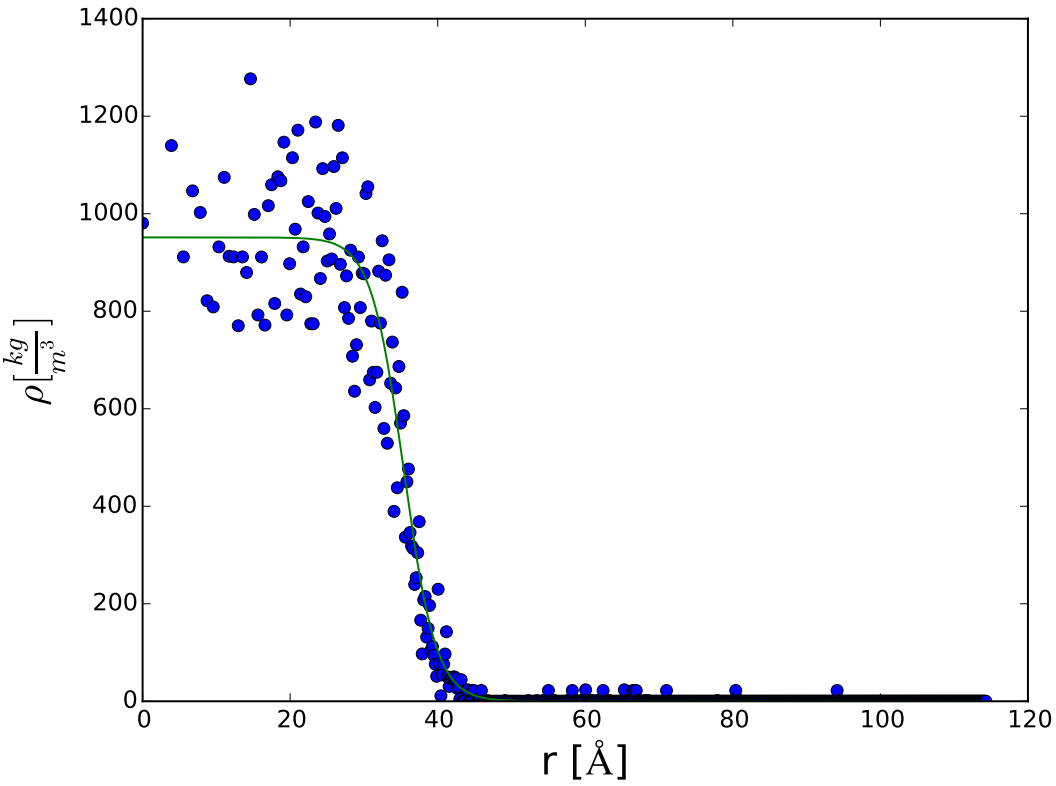

Figure 3.7: Droplet radial density profile.

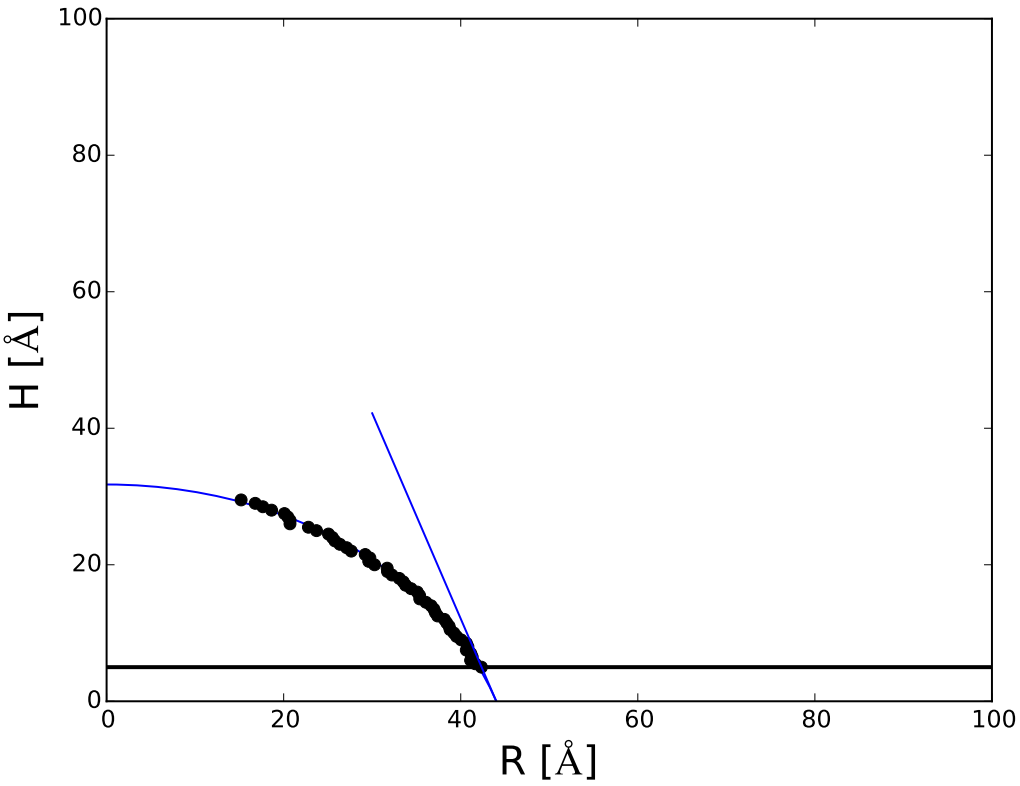

Figure 3.8: Droplet contact angle visualization.

3.3 Pool boiling simulation design

Simulation domain for calculation of pool boiling heat transfer coefficient is presented in Fig. 3.9. There are 5 distinct regions:

- Region 1 : Filled with water molecules that are not thermostated during the simulation. Those water molecules interact with the whole system and are free to move into and out of region 2 and 5.

- Region 2 : Filled with water molecules that are thermostated during entire simulation. Molecules in this region are kept at saturation temperature corresponding to chosen pressure. They are bounded inside this region and cannot leave region 2. This region is stimulating the bulk of the liquid at saturation and act as a heat sink in the system.

- Region 3 : Composed of copper atoms thermostated throughout the simulation. Atoms are kept at temperature corresponding to temperature of the wall of the heater.

- Region 4 : Rest of the wall is filled with copper atoms. The updating of the position of those atoms is not performed to decrease computational effort of the simulation.

- Region 5 : Vacuum. Empty space was left around the simulation box. The main purpose is to allow the particles of water to remain at saturation. During bubble formation water molecules are pushed from the space near the heater. Those molecules can than travel through region 2 to region 5.

The simulation was performed for water at pressure p=2.7bar. The bulk of the water was kept at saturation temperature through the entirety of the simulation. Timestep

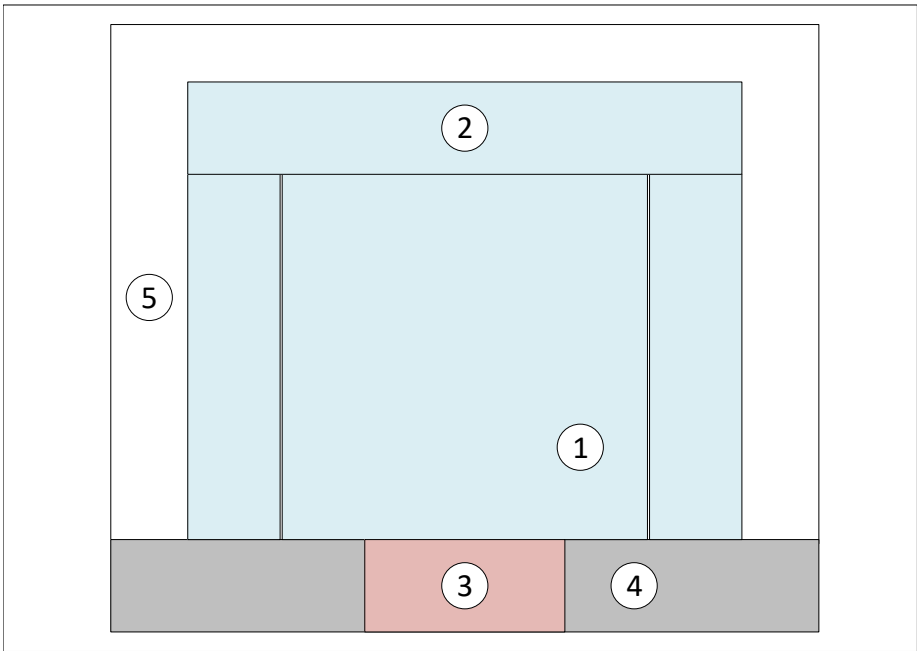

Figure 3.9: Experimental setup for Heat transfer coefficient for pool boiling simulation

chosen for the simulation is 0.5fs. The simulation was brought to equilibrium in the following steps. First, positions of all water molecules from region 1 and 2 were updated under NVT ensemble to saturation temperature for 15000 timestep. Next, the atoms in the heater were equilibrated for the same amount of time with NVT ensemble at temperature corresponding to wall temperature. Then, all atoms (excluding atoms in region 4) were updated with change of ensemble for region 1 from NVT to NVE. The simulations was performed until the heat flux from heater region and temperature of atoms in the region 1 was stable. The time required to run the simulation varied depending on the temperature of the wall superheat. On average

about 2 200 000 to 2 500 000 timesteps were required to collect the results. The simulation was limited in the availability of computational time. The convergence behaviour for each simulation is presented in Fig. 3.11 to 3.14. Presented values are average value from 500 timesteps. The vertical line indicates values that were used to calculate estimate of heat flux. Horizontal line indicates mean value of the heat flux.

Due to large variance of heat transfer measurement and unclear point where system achieves equilibrium, following rule was chosen to determine starting point of data acquisition. System was said to be at equilibrium when the difference between temperature of water in region 1 at the last time step and current step was lower then $0.2K$. The exception was made for $\Delta T = 30$ where system did not thermalize as quickly and limiting value of $0.1K$ was applied.

3.4 Heat transfer coefficient results

Heat transfer coefficient was calculated according to Eq. 3.4, where q represents heat transfer and ΔT wall superheat.

$$h = \frac{q}{\Delta T} \tag{3.4}$$

The comparison of correlations and MD results is presented in Table 3.6.

The ratio of MD simulation heat transfer coefficient and correlations is presented in Table 3.7.

Fig. 3.10 presents boiling curves for pool boiling. Comparison of some of the existing correlations with MD simulation is presented. It can be observed that MD

Table 3.6: Comparison of MD results and correlations for pool boiling. The subscript corresponds to different correlations: G - Gorenflo, C - Cooper, M - Mostinski

ΔT[K]	$h_{MD}[\frac{W}{m^2K}]$	$h_C^G[\frac{W}{m^2K}]$	$h_C^C[\frac{W}{m^2K}]$	$h_C^M[\frac{W}{m^2K}]$
10	$1.64 \cdot 10^5$	$9.25 \cdot 10^3$	$1.73 \cdot 10^4$	$1.56 \cdot 10^4$
20	$4.33 \cdot 10^6$	$7.01 \cdot 10^4$	$7.05 \cdot 10^4$	$7.86 \cdot 10^4$
30	$4.75 \cdot 10^6$	$2.29 \cdot 10^5$	$1.60 \cdot 10^5$	$2.02 \cdot 10^5$
40	$1.08 \cdot 10^7$	$5.32 \cdot 10^5$	$2.88 \cdot 10^5$	$3.96 \cdot 10^5$

Table 3.7: Comparison of ratio of MD HTC and correlations for pool boiling. The subscript corresponds to different correlations: G - Gorenflo, C - Cooper, M - Mostinski

ΔT[K]	$\frac{h_{MD}}{h_C^G}$	$\frac{h_{MD}}{h_C^C}$	$\frac{h_{MD}}{h_C^M}$
10	17.73	9.48	10.51
20	61.77	61.42	55.09
30	20.74	29.69	23.52
40	20.3	37.5	27.27

simulation overestimates the heat transfer coefficient for all the wall temperature values. The general trend of heat flux calculated from MD simulation is the same as existing correlations. For temperature difference $\Delta T = 20K$ significantly higher discrepancy can be observed. This may be explained by convergence not being achieved for this temperature value. Due to limited computational resources the simulation was performed for a fixed amount of time. It can be seen from convergence for each simulation that values of heat transfer vary significantly. Additionally, estimate of heat flux value is influenced by autocorrelation of heat flux values.

The bubble formation on the heating surface was observed for all wall temperatures. The process of bubble creation is presented in Fig. 3.15 for wall superheat $\Delta T = 20K$. After achieving size corresponding to temperature of heater wall, bubble shape fluctuated but remained mostly constant in size. Bubble detachment was not observed due to short time of simulation performed. Additionally, the special design of the simulation with some of the particles of water trapped in region 2 may have further hinder this process. The bubble size was dependent on temperature of the heater wall. Visualization of bubble size are presented in Fig. 3.16 for $\Delta T = [5, 10, 20]K$. It can be observed that bubble size is increasing with increasing temperature. This is consistent with water molecules having higher energy.

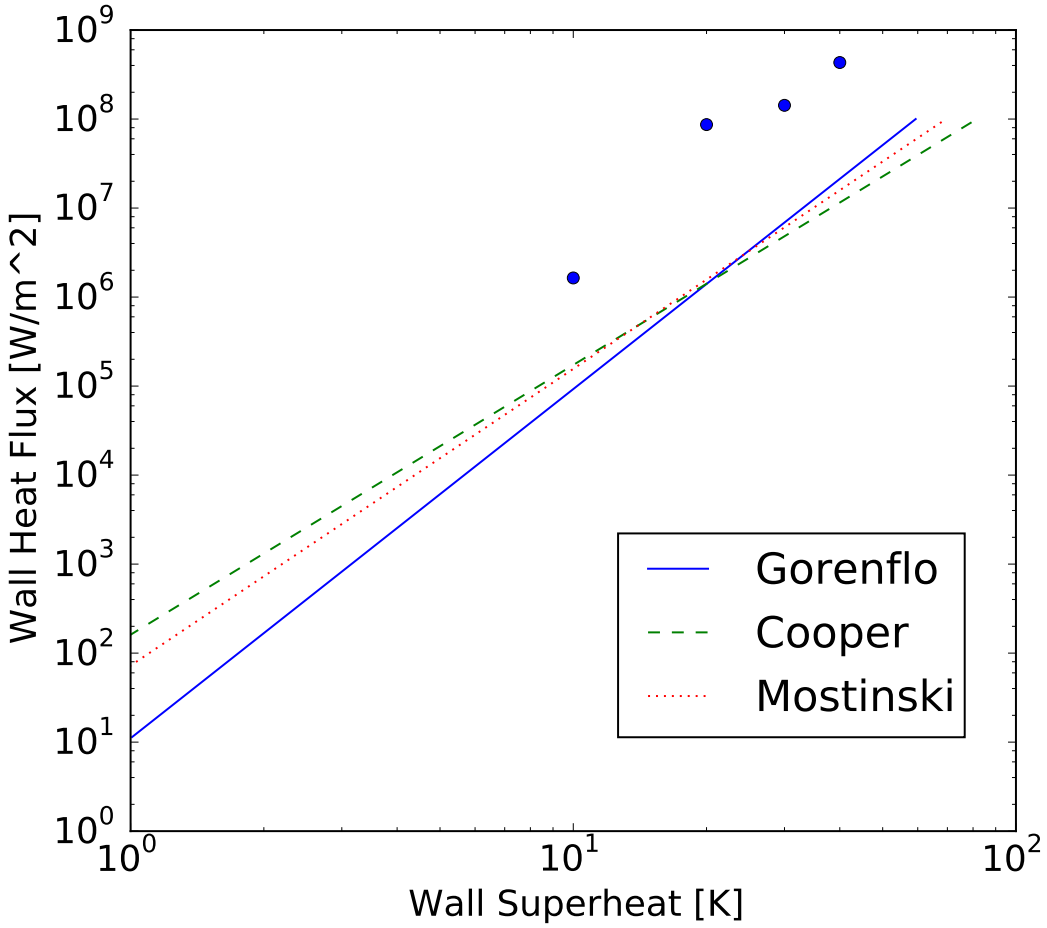

Figure 3.10: Pool boiling curve for water at 2.7bar. The figure presents comparison of existing correlations for pool boiling curve and results of simulation for $\Delta T = [10, 20, 30, 40]K$.

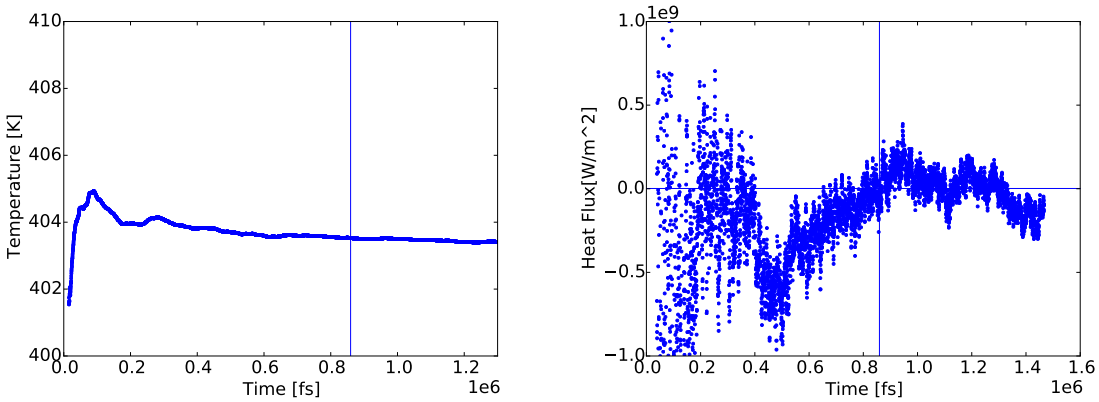

Figure 3.11: Temperature and heat flux convergence for $\Delta T = 10K$.

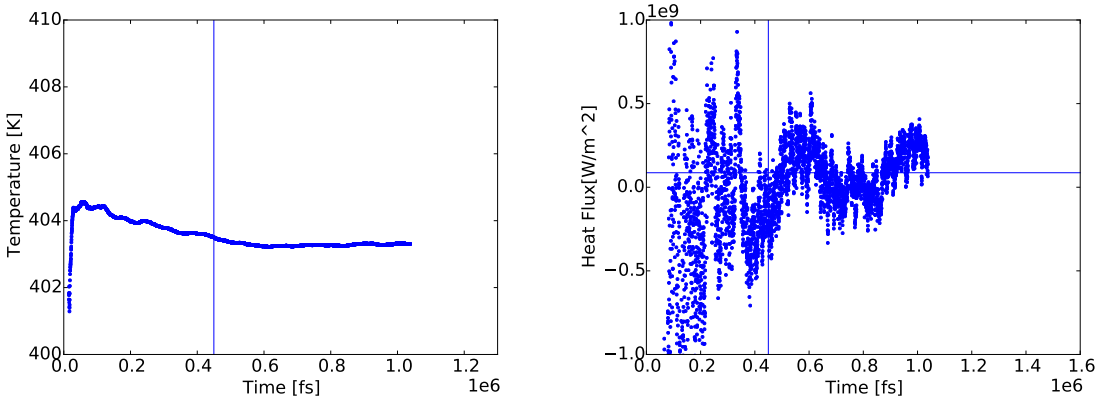

Figure 3.12: Temperature and heat flux convergence for $\Delta T = 20K$.

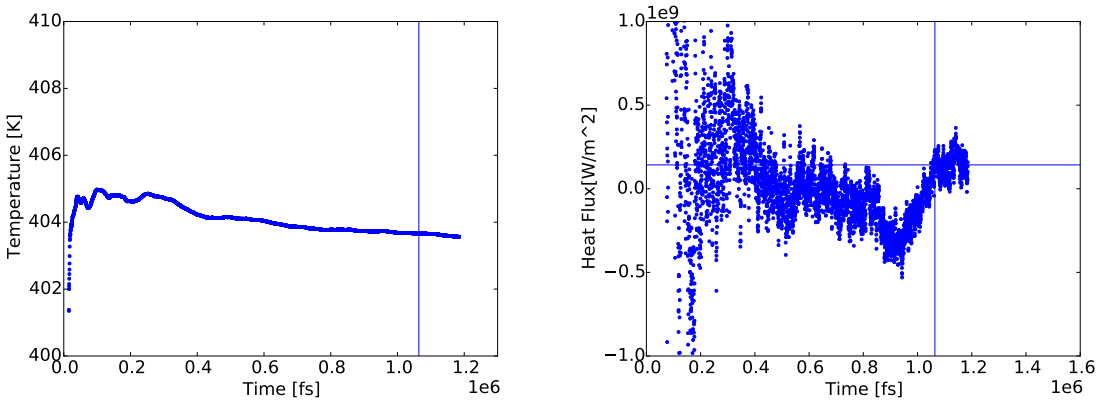

Figure 3.13: Temperature and Heat flux convergence for $\Delta T = 30K$.

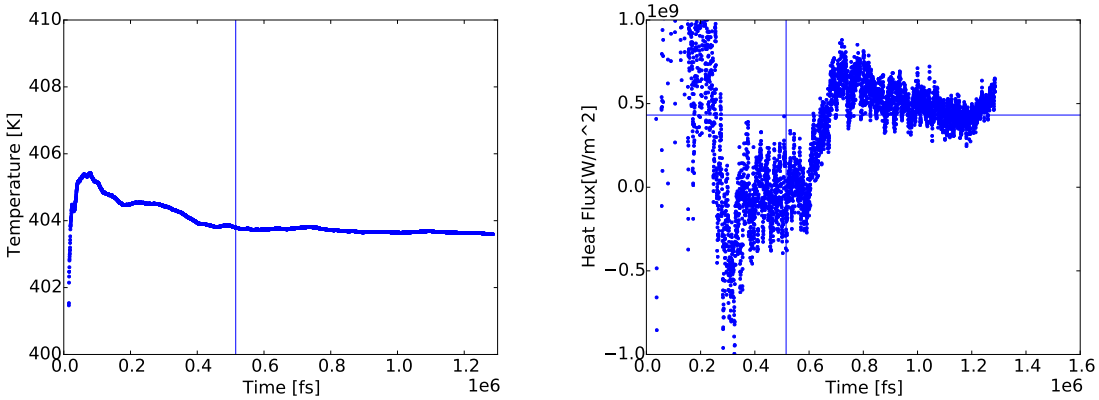

Figure 3.14: Temperature and Heat flux convergence for $\Delta T = 40K$.

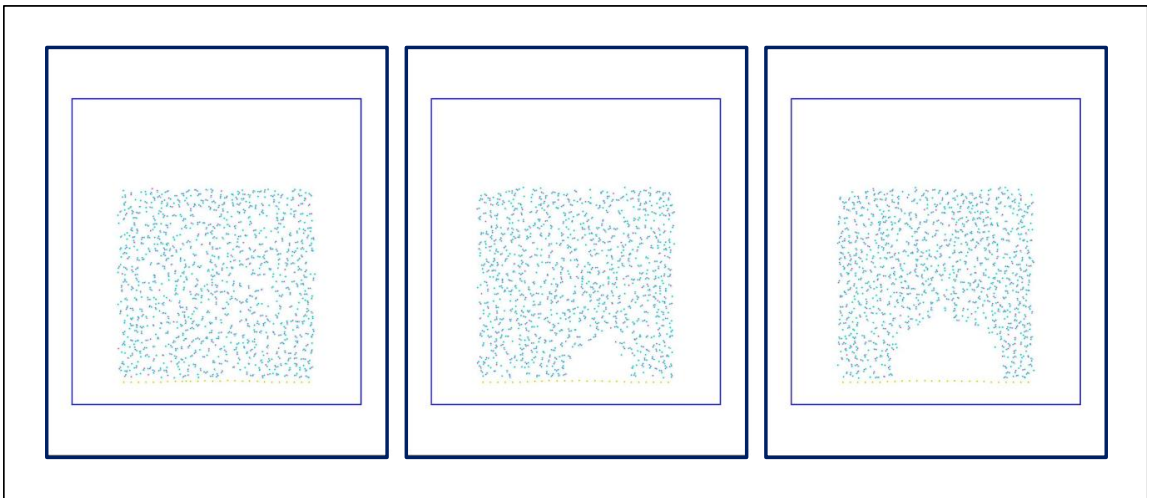

Figure 3.15: Bubble formation for$\Delta T = 20K$.

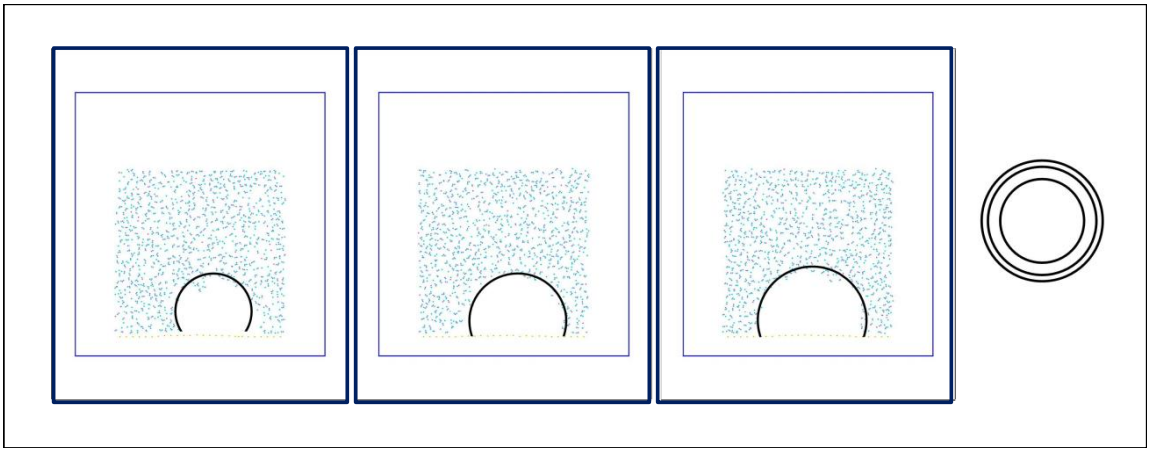

Figure 3.16: Bubble size comparison from the left $\Delta T = [5, 10, 20]K$. On the right relative difference between bubble sizes was visualized.

Chapter 4

Conclusions

Analysis illustrates application of molecular dynamic simulation to calculation of macroscopic properties. It was shown that model TIP4P is capable of accurate prediction of water properties. Accurate simulation of liquid water and vapor density was presented. Surface tension results from MD simulation deviate from experimental results by 10% on average. Nevertheless, the temperature dependence of surface tension is consistent with experimental data and increasing number of atoms and time of the simulation would give more accurate results, as illustrated in [33].

Simulation evaluating contact angle was performed. Potential describing water - copper interaction was parametrized to match contact angle for water droplet on copper plate. The value of contact angle at $T = 100^oC$ matched well. It is worth mentioning that the contact angle is dependent on the size of the droplet in MD simulation [31] and potential that was used is only an approximation of real interaction potential. Chosen potential that was identified to give contact angle comparable to experimental value is not unique, as there are more than one parameter to fit and only one experiment. Additional simulations are needed to find more accurate interaction potential. For example, simulation of water molecule orientation on the solid surface can be performed and compared with experimental results. This simu-

lation was not performed due to simplicity of L-J potential, which is unable to model required physics of the phenomenon.

Using selected potentials, pool boiling heat transfer coefficient was calculated. Special setup was created to simulate large pool of water. The results cannot be compared to experimental data, due to low number of water molecules used and short time of the simulation. For example, copper plate was modelled with 6 layers of copper atoms which made it impossible to madel any types of surface effects, such as surface roughness. Additionally, time of the simulation was not adequate to observe bubble detachment. Calculated heat transfer coefficient gave higher heat flux than predicted by correlation by one order of magnitude. Nevertheless, the general trend was the same between simulation and correlations.

The potential applied in the simulation, especially for water - copper interaction, does not accurately represent the interaction potential. More accurate interaction model needs to be developed that would model the induction of charges in the copper plate by water molecules. Additionally, the convergence study should be improved, it was limited due to large computational effort.

Vapor bubble was created for all values of wall superheat. Furthermore, the dependence of the size of vapor bubble on wall temperature superheat was observed. However, bubble detachment was not observed in the simulation due to small simulation size and temporal limitation of the study.

The analysis was performed to investigate the feasibility of MD simulation in the study of boiling process and not to get accurate prediction of pool boiling heat transfer coefficient. Simulation of the pool boiling, limited by size and time con-

straints, was presented with the use of existing potentials. For accurate prediction of heat transfer coefficient new interaction potentials need to be developed. Additionally, simulation size and time need to be increased significantly. With growing computational resources and improvement in description of molecular potentials, MD simulations can become valuable tool for in the study of boiling process as it is capable of analysis on molecular level.

4.1 Further work

To improve the simulation accuracy, following steps can be undertaken:

- Improving the interaction potential between water molecules and copper atoms. More appropriate choice of potential form can be used capable of modelling induction of charges by water molecules.
- Increasing domain size.
- Increasing time of the simulation, especially for higher values of temperature.
- Convergence study is necessary to determine if time step used is adequate for the analysis.
- Contact angle calculation can be performed considering dependence of contact angle on the droplet size.

References

[1] J. L. F. ABASCAL and C. VEGA, "A general purpose model for the condensed phases of water: TIP4P/2005," *The Journal of Chemical Physics*, **123**, *23*, 234505 (2005).

[2] S. PLIMPTON, "Fast Parallel Algorithms for Short-Range Molecular Dynamics," *Journal of Computational Physics*, **117**, *1*, 1 – 19 (1995).

[3] "LAMMPS Molecular Dynimic Simulator," .

[4] A. FAGHRI, Y. ZHANG, and J. R. HOWELL, *Advanced Heat and Mass Transfer*, Global Digital Press (2010).

[5] M. KARPLUS and G. A. PETSKO, "Molecular dynamics simulations in biology," *Nature*, **347**, 631 – 639 (1990).

[6] D. E. H. JR., "Application of molecular dynamics simulations to the study of ion-bombarded metal surfaces," *Critical Reviews in Solid State and Materials Sciences*, **14**, *sup1*, s1–s78 (1988).

[7] S. GE, Y. GU, and M. CHEN, "A molecular dynamics simulation on the convective heat transfer in nanochannels," *Molecular Physics*, **113**, *7*, 703–710 (2015).

[8] J. WANG and T. HOU, "Application of Molecular Dynamics Simulations in Molecular Property Prediction. 1. Density and Heat of Vaporization," *Journal of Chemical Theory and Computation*, **7**, *7*, 2151–2165 (2011), pMID: 21857814.

[9] J. WANG and T. HOU, "Application of molecular dynamics simulations in molecular property prediction II: Diffusion coefficient," *Journal of Computational Chemistry*, **32**, *16*, 3505–3519 (2011).

[10] G. J. WAGNER, "Atomistic-to-Continuum Coupling Methods for Heat Transfer in Solids," pp. 3–20 (03 2013).

[11] L. J. LABERGE and J. C. TULLY, "A rigorous procedure for combining molecular dynamics and Monte Carlo simulation algorithms," *Chemical Physics*, **260**, *1*, 183 – 191 (2000).

[12] "TRACE V5. 0 Theory ManualField Equations, Solution Methods, and Physical Models," Tech. rep., U. S. NRC (2010).

[13] D. POULIKAKOS, S. ARCIDIACONO, and S. MARUYAMA, "Molecular Dynamics Simulations in Nanoscale Heat Transfer: A Review, Micro. Thermophys," *A Review, Micro. Thermophys. Eng*, pp. 181–206 (2003).

[14] M. J. P. NIJMEIJER, A. F. BAKKER, C. BRUIN, and J. H. SIKKENK, "A molecular dynamics simulation of the LennardJones liquidvapor interface," *The Journal of Chemical Physics*, **89**, *6*, 3789–3792 (1988).

[15] M. MECKE, J. WINKELMANN, and J. FISCHER, "Molecular dynamics simulation of the liquidvapor interface: The Lennard-Jones fluid," *The Journal of Chemical Physics*, **107**, *21*, 9264–9270 (1997).

[16] M. ORSI, "Comparative assessment of the ELBA coarse-grained model for water," *Molecular Physics*, **112**, *11*, 1566–1576 (2014).

[17] Y. LEI and Y. LENG, "Molecular dynamics simulations on the phase transition of simple non-polar fluids under nanometre confinement," *Proceedings of the Institution of Mechanical Engineers, Part N: Journal of Nanoengineering and Nanosystems*, **224**, *1-2*, 69–77 (2010).

[18] S. K. DAS, S. U. S. CHOI, and H. E. PATEL, "Heat Transfer in Nanofluids - A Review," *Heat Transfer Engineering*, **27**, *10*, 3–19 (2006).

[19] S. SARKAR and R. P. SELVAM, "Molecular dynamics simulation of effective thermal conductivity and study of enhanced thermal transport mechanism in nanofluids," *Journal of Applied Physics*, **102**, *7*, 074302 (2007).

[20] A. HENS, R. AGARWAL, and G. BISWAS, "Nanoscale study of boiling and evaporation in a liquid Ar film on a Pt heater using molecular dynamics simulation," *International Journal of Heat and Mass Transfer*, **71**, *Supplement C*, 303 – 312 (2014).

[21] S. PARK, J. WENG, and C. TIEN, "A molecular dynamics study on surface tension of microbubbles," *International Journal of Heat and Mass Transfer*, **44**, *10*, 1849 – 1856 (2001).

[22] H. OKUMURA and N. ITO, "Nonequilibrium molecular dynamics simulations of a bubble," *Phys. Rev. E*, **67**, 045301 (Apr 2003).

[23] Y. TANG, T. FU, Y. MAO, Y. ZHANG, and W. YUAN, "Molecule Dynamics Simulation of Heat Transfer Between Argon Flow and Parallel Copper Plates," **5**, *3* (Aug 2014).

[24] X. YIN, M. BAI, C. HU, and J. LV, "MOLECULAR DYNAMICS SIMULATION ON THE POOL BOILING HEAT TRANSFER OF NANOFLUIDS," *Nanoscale Res Lett*, **6** (2011).

[25] H. INAOKA and N. ITO, "Numerical simulation of pool boiling of a Lennard-Jones liquid," *Physica A: Statistical Mechanics and its Applications*, **392**, *18*, 3863 – 3868 (2013).

[26] N. ATTIG, *Computational Soft Matter: from Synthetic Polymers to Proteins: Lecture notes.*, NIC series, NIC (2004).

[27] D. GORENFLO, *Pool Boiling*, VDI Verlag, Dusseldorf (1993).

[28] M. COOPER, "Heat Flow Rates in Saturated Nucleate Pool Boiling-A Wide-Ranging Examination Using Reduced Properties," **16**, 157–239 (12 1984).

[29] I. L. MOSTINSKI, "Application of the Rule of Corresponding States for Calculation of Heat Transfer and Critical Heat Flux to Boiling Liquids," *British Chemical Engineering Abstracts*, **580**, *150* (1963).

[30] F. H. STILLINGER and A. RAHMAN, "Improved simulation of liquid water by molecular dynamics," *The Journal of Chemical Physics*, **60**, *4*, 1545–1557 (1974).

[31] T. WERDER, J. H. WALTHER, R. L. JAFFE, T. HALICIOGLU, and P. KOUMOUTSAKOS, "On the WaterCarbon Interaction for Use in Molecular Dynamics Simulations of Graphite and Carbon Nanotubes," *The Journal of Physical Chemistry B*, **107**, *6*, 1345–1352 (2003).

[32] A. P. BOYES and A. B. PONTER, "Wettability of copper and polytetrafluoroethylene surfaces with waterthe influence of environmental conditions," *Chemie Ingenieur Technik*, **45**, *21*, 1250–1256 (1973).

[33] J. ALEJANDRE and G. A. CHAPELA, "The surface tension of TIP4P/2005 water model using the Ewald sums for the dispersion interactions," *The Journal of Chemical Physics*, **132**, *1*, 014701 (2010).